Molecular Cell, Vol. 11, 1445–1456, June, 2003, Copyright ©2003 by Cell Press

Structure of a β-TrCP1-Skp1-β-Catenin Complex: Destruction Motif Binding and Lysine Specificity of the $SCF^{\beta\text{-}TrCP1}$ Ubiquitin Ligase

Geng Wu,[1,2] Guozhou Xu,[1]
Brenda A. Schulman,[1,4] Philip D. Jeffrey,[1]
J. Wade Harper,[3] and Nikola P. Pavletich[1,2,*]
[1]Cellular Biochemistry and Biophysics Program and
[2]Howard Hughes Medical Institute
Memorial Sloan-Kettering Cancer Center
New York, New York 10021
[3]Verna and Marrs McLean Department
of Biochemistry and Molecular Biology and
Howard Hughes Medical Institute
Baylor College of Medicine
Houston, Texas 77030

Summary

The SCF ubiquitin ligases catalyze protein ubiquitination in diverse cellular processes. SCFs bind substrates through the interchangeable F box protein subunit, with the >70 human F box proteins allowing the recognition of a wide range of substrates. The F box protein β-TrCP1 recognizes the doubly phosphorylated DpSGϕXpS destruction motif, present in β-catenin and IκB, and directs the $SCF^{\beta\text{-}TrCP1}$ to ubiquitinate these proteins at specific lysines. The 3.0 Å structure of a β-TrCP1-Skp1-β-catenin complex reveals the basis of substrate recognition by the β-TrCP1 WD40 domain. The structure, together with the previous SCF^{Skp2} structure, leads to the model of SCF catalyzing ubiquitination by increasing the effective concentration of the substrate lysine at the E2 active site. The model's prediction that the lysine-destruction motif spacing is a determinant of ubiquitination efficiency is confirmed by measuring ubiquitination rates of mutant β-catenin peptides, solidifying the model and also providing a mechanistic basis for lysine selection.

Introduction

Ubiquitin-mediated proteolysis has a regulatory function in many diverse cellular processes (Hershko and Ciechanover, 1998). The ubiquitination of a specific protein is carried by the ubiquitin-protein ligases (also known as E3s), which act at the last step of a three-enzyme cascade involving ubiquitin-activating (E1) and ubiquitin-conjugating enzymes (E2). The E1 activates the ubiquitin in an ATP-dependent reaction and transfers it to the E2 through the formation of a thioester bond between the E2 active site cysteine and the ubiquitin C terminus. The E3 binds both a cognate E2 and the substrate, and is responsible for conferring substrate specificity to the ubiquitination reaction (reviewed in Pickart, 2001). The binding of the E3 to the substrate protein is also the primary event regulating protein stability and is in many cases governed by the phosphorylation or other post-translational modification of the substrate. E3s are a diverse family of proteins and protein complexes, and they mediate ubiquitination in at least two distinct ways. HECT-type E3s first form an E3-ubiquitin thioester conjugate and then transfer the ubiquitin to the substrate. RING-type E3s, which are characterized by the presence of a RING domain that binds the E2, do not form an E3-ubiquitin conjugate, and they are thought to promote the ubiquitination of the substrate directly by the E2 (reviewed in Pickart, 2001).

The SCF is a four-subunit RING-type E3, and it represents the largest family of E3s known to date (Deshaies, 1999). SCF family members regulate the cell division cycle, transcriptional pathways, and multiple aspects of development, and they also play a central role in the phosphorylation-mediated destruction of regulatory proteins. SCF complexes are composed of the scaffold protein Cul1, the RING-domain protein Rbx1/Roc1, the adaptor protein Skp1, and an F box protein that binds the substrate. Rbx1 associates with Cul1 and the E2 (Skowyra et al., 1999), while Skp1 interacts simultaneously with Cul1 and with the F box protein (Bai et al., 1996; Feldman et al., 1997; Skowyra et al., 1997). F box proteins constitute the largest known class of E3 specificity components. Human and mouse genomes contain more than 70 F box proteins while *C. elegans* contains 326 predicted F box proteins (Winston et al., 1999b; Kipreos and Pagano, 2000; J.W.H and J. Jin, unpublished data). F box proteins interact with Skp1 through the ~40 amino acid F box motif (Bai et al., 1996; Schulman et al., 2000) and with substrates through C-terminal protein-protein interaction domains, including WD40 repeats (Fbw subfamily) and leucine-rich repeats (LRRs; Fbl subfamily) (Deshaies, 1999). In addition to this original SCF family, there is at least one other family of SCF-like ubiquitin ligase complexes that are composed of the Cul1-paralogue Cul2, Rbx1, the Skp1-like adaptor protein ElonginC, and a SOCS box protein. SOCS box proteins are structurally and functionally related to F box proteins (Stebbins et al., 1999; Schulman et al., 2000), and the SOCS box protein VHL has been shown to bind to the hypoxia-inducible transcription factor 1-α (Hif1-α) and promote its ubiquitination by the SCF-like ubiquitin ligase (Ivan and Kaelin, 2001).

Much of our understanding of SCF function and the role of phosphorylation in protein turnover has come from the analysis of the WD40 repeat containing F box protein β-TrCP1, which is conserved from *C. elegans* to humans. β-TrCP1 has been biochemically and genetically demonstrated to control the stability of proteins involved in transcription, including β-catenin (Hart et al., 1999; Latres et al., 1999) and IκB (Li and Verma, 2002). All known $SCF^{\beta\text{-}TrCP1}$ substrates contain the DSGϕXS destruction motif (ϕ representing a hydrophobic and X any amino acid). Phosphorylation of both serines of the destruction motif is a prerequisite for β-TrCP1 binding, linking phosphorylation-mediated signaling to protein ubiquitination and destruction. In the case of IκB, which holds the transcription factor NFκB in an inactive cyto-

*Correspondence: nikola@xray2.mskcc.org
[4]Present address: Departments of Structural Biology and Tumor Cell Biology, St. Jude Children's Research Hospital, Memphis, Tennessee 38105.

plasmic complex, cytokines induce the phosphorylation of the two serine residues (Ser32 and Ser36) in the IκB destruction motif, leading to its ubiquitination by $SCF^{\beta\text{-}TrCP1}$, destruction by the proteasome, and liberation of NFκB (Winston et al., 1999a; Yaron et al., 1998; Li and Verma, 2002). By contrast, the phosphorylation of the destruction motif of β-catenin (Ser33 and Ser37) by the GSK3β-APC-Axin complex occurs in the absence of Wnt signals (Hart et al., 1999; Latres et al., 1999; Winston et al., 1999a). Wnt signals block β-catenin phosphorylation, leading to its stabilization, translocation to the nucleus, and transcriptional activation of proliferation-associated genes (Polakis, 1999). Tumor-derived mutations in APC or in β-catenin, which are among the most common mutations in colon cancer, prevent β-catenin ubiquitination (Polakis, 1999).

It has been proposed that the SCF and other RING-E3s catalyze ubiquitination through a mechanism that involves the recruitment and productive positioning of the substrate relative to the E2 active site (Schulman et al., 2000; Zheng et al., 2000, 2002). This model emerged, in part, from the structures of the Cul1-Rbx1-Skp1-F box^{Skp2} complex (Zheng et al., 2002), of the LRR-containing F box protein Skp2 bound to Skp1 (Schulman et al., 2000), of the VHL-ElonginC-ElonginB complex bound to a Hif1α substrate peptide (Stebbins et al., 1999; Min et al., 2002; Hon et al., 2002), and of the RING E3 c-Cbl bound to an E2 (Zheng et al., 2000). These structures revealed that individual E3 subunits and domains are connected through rigid structural couplings without any flexible linkages and, together with mutagenesis (Zheng et al., 2002), also helped eliminate the alternative mechanism of acid/base catalysis by E3 residues. General aspects of the positioning model have been supported by several mutagenesis studies. The introduction of flexible linkers that eliminate the rigidity of the Cul1 scaffold was shown to inactivate the SCF^{Skp2} without affecting its ability to bind the substrate or the E2 (Zheng et al., 2002). Mutation of a Skp1 residue important for the precise arrangement of the Skp1-Skp2 interface was shown to disrupt Skp1 function in yeast without abolishing Skp1-Skp2 binding (Schulman et al., 2000). Mutations in c-Cbl that affect the rigid linkage between the E2 and substrate binding domains abolished its function without significantly affecting its ability to bind either substrate or E2s (Joazeiro et al., 1999). In addition, VHL residues important for the relative arrangement of its α and β domains, which bind the ElonginC adaptor and the Hif1α substrate, respectively, were found to be frequently mutated in the von Hippel Lindau cancer-predisposition syndrome (Stebbins et al., 1999). Further supporting the positioning model of catalysis, the structure of yeast Skp1 bound to the WD40-containing F box protein Cdc4, reported when this manuscript was first submitted, also showed rigid coupling between the F box and substrate binding domain, and Cdc4 mutations designed to affect the rigid coupling disrupted function in vivo (Orlicky et al., 2003).

To further elaborate on the mechanistic details of this model and to understand the substrate specificity of the $SCF^{\beta\text{-}TrCP1}$, we have determined the 3.0 Å crystal structure of the human β-TrCP1-Skp1 complex bound to a 26 residue β-catenin substrate peptide. The structure, in conjunction with measurements of in vitro ubiquitination rates of mutant β-catenin peptides, leads to the refined model that the SCF catalyzes ubiquitination by increasing the effective concentration of the substrate lysine at the E2 active site, and also provides a mechanism for the selection of lysine(s).

Results and Discussion

Overall Structure of the β-TrCP1-Skp1-β-Catenin Complex

The β-TrCP1-Skp1 complex was produced in insect cells by coexpressing human Skp1 with a human β-TrCP1 fragment (residues 139 to 569) that lacks a 138 residue N-terminal portion of unknown function. This complex was crystallized bound to a 26 amino acid human β-catenin substrate peptide (residues 19 to 44) that gets ubiquitinated by the $SCF^{\beta\text{-}TrCP1}$ in vitro.

The Skp1-β-TrCP1-β-catenin complex has an elongated, curved structure, with Skp1 and the β-catenin peptide located at opposite ends. β-TrCP1 consists of the N-terminal F box domain (residues 139 to 186), a C-terminal WD40-repeat domain (residues 253 to 545), and an α-helical domain (residues 187 to 252; hereafter linker domain) linking the two (Figures 1A–1C). The β-TrCP1 F box motif has the same overall three-helix cluster structure seen with Skp2 (Schulman et al., 2000) but shows considerable variation in its amino- and carboxy-terminal regions. The seven WD40 repeats form a torus-like structure (named β propeller) that is characteristic of this fold (Wall et al., 1995). The β-TrCP1 β propeller is very similar to the canonical β propeller structure, and it can be superimposed on the WD40 domains of Gβ (Wall et al., 1995) and Tup1 (Sprague et al., 2000) with root-mean-square deviations (rmsd) of 1.5–1.6 Å over 255 Cα atoms. The β-TrCP1 linker domain consists of four α helices, and it interacts extensively with both the F box and with one face of the WD40 β propeller. Skp1, previously shown to have a BTB/POZ fold structure followed by two helices (H7 and H8), binds the β-TrCP1 F box in a manner similar to the Skp1-Skp2 complex (Schulman et al., 2000).

The β-catenin peptide binds to one face of the β propeller, opposite from where the linker packs (Figures 1A and 1B). Of the 26 β-catenin residues in the crystals, only an 11 residue segment (residues 30 to 40), centered on the doubly phosphorylated destruction motif (residues 32 to 37), is ordered in the structure. The phosphoserine, aspartic acid, and hydrophobic residues of the destruction motif are recognized directly by contacts from β-TrCP1.

β-Catenin Binding

As seen with other WD40 domain structures, the β-TrCP1 β propeller has a narrow channel running through the middle of the torus-like structure (Figure 1B), with the channel being narrowest near the top face (convention of Wall et al., 1995). The β-catenin peptide binds the top face of the β propeller, with the six residue destruction motif dipping into the central channel (Figures 2A and 2B). The middle portion of the peptide has an extended conformation, and the two ends have turn-like conformations. All seven WD40 repeats of β-TrCP1 contribute contacts to β-catenin. Two-thirds of the contacts involve the A strands that line the central channel and the rest of the BC loops (Figure 1B).

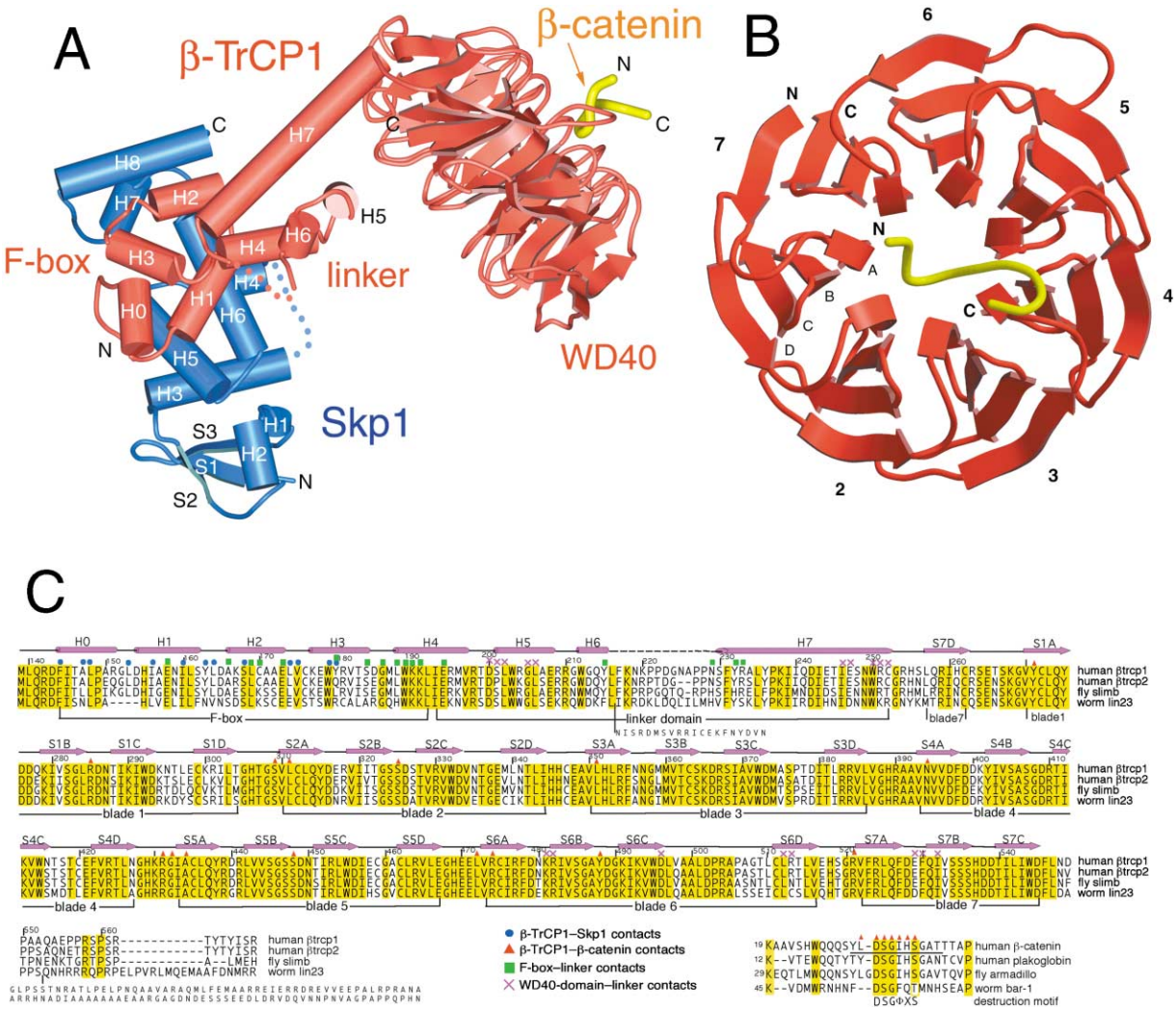

Figure 1. Structure of the Skp1-β-TrCP1-Phosphorylated β-Catenin Peptide Complex

(A) Overall view of the complex. β-TrCP1 is colored red, Skp1 blue, and β-catenin yellow. The secondary structure elements for Skp1 and for the F box and linker domains of β-TrCP1 are labeled. Dotted lines represent disordered regions. Figures were prepared with the programs MOLSCRIPT (Kraulis, 1991), GL_RENDER, and POVRAY (L. Essar, personal communication).

(B) The phosphorylated β-catenin peptide binds to the top face of the WD40 domain of β-TrCP1, and it partially dips into the central channel. The seven blades of the WD40 domain are numbered from 1 to 7, and the strands within each blade are named A to D according to the convention of Wall et al. (1995).

(C) Top panel: Sequence conservation and secondary structure elements of human β-TrCP1 (residues 139 to 569), with dashed lines indicating regions that are disordered in the crystal structure. Residues identical in all four orthologs are highlighted in yellow. β-TrCP1 residues that interact with Skp1 are indicated by blue dots and with β-catenin by red triangles. β-TrCP1 residues that mediate F box-linker interactions are indicated by green rectangles, and those mediating WD40 domain-linker interactions by purple crosses. Bottom panel: Sequence conservation of the human β-catenin peptide (residues 19 to 44) used in crystallization. The consensus destruction motif is shown below the alignment, with ϕ representing a hydrophobic residue and X any residue. β-TrCP1-interacting residues of β-catenin are indicated by red triangles. The β-catenin residues that have clear electron density in the crystal structure are underlined.

Nearly all of the β-TrCP1 contacts are made by the six residue destruction motif (Figure 2A). The side chains of Asp32, Gly34, and Ile35, and the backbone amide and carbonyl groups of His36 insert the farthest into the channel, making intermolecular contacts in a mostly buried environment. The phosphate groups of pSer33 and pSer37 bind sites at the rim, at opposite sides of the channel, and their contacts are partially solvent exposed.

The phosphate group of pSer33 makes the largest number of contacts, forming hydrogen bonds with the side chain hydroxyl groups of Tyr271, Ser309, and Ser325, and electrostatic interactions with the guanidinium group of Arg285 (Figure 2A). In addition, the backbone amide of pSer33 also hydrogen bonds to the Tyr271 hydroxyl group, creating a hydrogen bond network. The phosphate group of pSer37 contacts fewer residues, forming hydrogen bonds with the hydroxyl group of Ser448 and the backbone amide group of Gly432, and electrostatic interactions with the guanidinium group of Arg431 (Figures 2A and 2B).

Among the buried β-catenin residues, Asp32, which

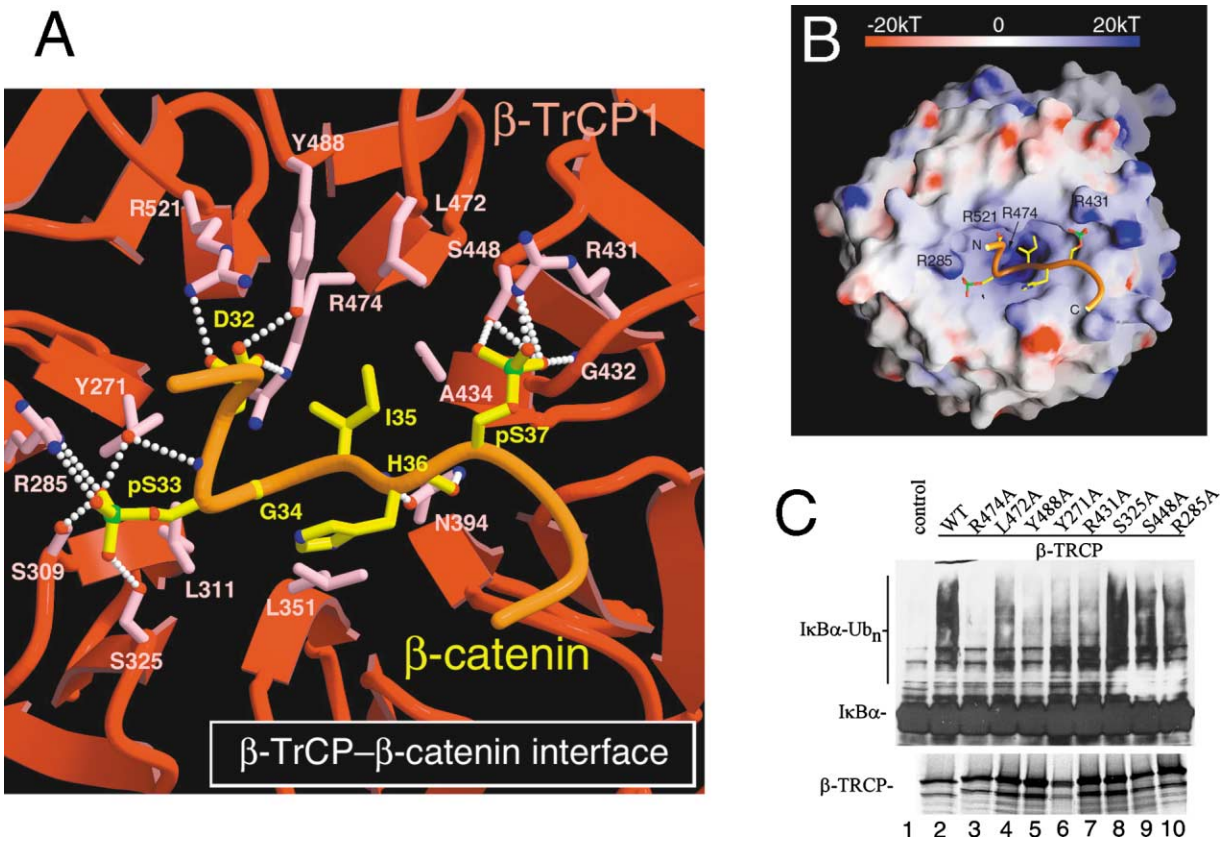

Figure 2. The Doubly Phosphorylated β-Catenin Peptide Binds to the Top Face of the β-TrCP1 WD40 Domain

(A) Close-up view of the interface between the β-TrCP1 WD40 domain and the doubly phosphorylated β-catenin peptide. The β-TrCP1 WD40 domain is shown in red, with its side chains in pink, and the β-catenin peptide is shown in orange, with its side chains in yellow. Hydrogen bonds are represented by white dotted lines.

(B) Surface representation of the top face of the β-TrCP1 WD40 domain with the β-catenin peptide bound. The surface is colored according to the electrostatic potential (−20 kT to +20 kT), calculated in the absence of β-catenin with the program GRASP.

(C) Mutational analysis of β-TrCP1 residues that interact with the destruction motif using an in vitro IκBα ubiquitination assay. The ubiquitination assays (upper panel) were performed using a panel of β-TrCP1 mutants (lanes 2–10) produced by in vitro translation in the presence of ^{35}S-methionine (lower panel). Control reactions (lane 1) contained unprogrammed reticulocyte extracts. IκBα and IκBα-ubiquitin conjugates were detected by immunoblotting with anti-IκBα antibodies.

is an invariant destruction motif residue, makes the most extensive contacts (Figure 2A). Its side chain makes a charge-stabilized hydrogen bond with Arg474 and another hydrogen bond with the hydroxyl group of Tyr488 of β-TrCP1. Gly34, also an invariant destruction motif residue, packs with Leu311 and Leu351 in an environment with little space for a nonglycine residue. Ile35, whose hydrophobic nature is conserved in the motif, makes van der Waals contacts with Ala434, Leu 472, and the aliphatic portion of the Arg474 side chain. The side chain of His36, which is in the only variable position of the motif, points outward and has no interactions with β-TrCP1, but its backbone amide and carbonyl groups make a pair of hydrogen bonds with the side chain of Asn394.

The two residues preceding the destruction motif point away from β-TrCP1, with only one contact, between the Leu31 backbone carbonyl group of β-catenin and the Arg521 guanidinium group of β-TrCP1, made in this region. Residues 38 to 40 following the motif form a turn that packs only loosely on the surface of the β-propeller.

Three Positions of the WD40 Motif Make the Majority of Contacts

The majority (14/15) of the β-TrCP1 residues that contact β-catenin are located at one of three positions of the WD40 repeat motif. The most common position, used by six of the seven repeats, is the second residue of the A strand (the A2 position; Figures 1B and 1C). The other two positions are the residue immediately prior to the start of the A strand (A-1 position), and the residue immediately after the B strand (B+1 position), each used by four repeats.

The use of three positions of the WD40 repeat for binding is similar to what has been observed in the binding of the transducin $G_t\beta\gamma$ to phosducin, which has a small helical domain that binds on the $G_t\beta$ propeller channel. Gaudet et al. (1996) noted that three residues of the WD40 motif are repeatedly involved in interactions with phosducin, and these are the same residues as the A-1, A2, and B+1 positions of the β-TrCP1 repeats. These similarities highlight the central channel as a structural scaffold that can adapt, through side chain

changes, to recognizing diverse secondary structure and sequence over short polypeptide stretches.

Remarkably, the phosphate groups of pSer33 and pSer37 bind to very similar sites on repeats 2 and 5, respectively, and they share contacts similar to the A-1 (Ser309 and Gly432) and B+1 (Ser325 and Ser448) positions of these repeats (Figure 2A). The additional contacts that pSer33 makes to the neighboring repeat 1 (A2 and B+1 positions) are not possible for pSer37 due to the steric hindrance by the β-catenin polypeptide backbone preceding pSer37. In the recently reported structure of the yeast Skp1-Cdc4 complex bound to a phosphopeptide selected from a library, the single phosphothreonine binds the Cdc4 WD40 domain in a location similar to that of pSer37, interacting with the A2 and B+1 positions of repeats 3 and 4 (Orlicky et al., 2003).

Mutational Analysis of β-TrCP1-Destruction Motif Recognition

To further explore β-TrCP1-destruction motif recognition, we mutated eight of the β-TrCP1 residues that contact the pSer33, pSer37, Asp32, and Ile36 residues of the destruction motif, and tested the ability of single-site β-TrCP1 mutants to promote the $SCF^{\beta\text{-}TrCP1}$-mediated polyubiquitination of IκBα in an in vitro translation system (Winston et al., 1999a) (Figure 2C). Mutation of Arg474 or Tyr488, both of which contact Asp32, to alanine had the biggest effect, resulting in complete loss of $SCF^{\beta\text{-}TrCP1}$ activity in this assay. Among the phosphoserine contacts, mutation of Arg431 and Tyr271 resulted in significant loss of activity. These findings support the structure-based conclusion that Asp32, pSer33, pSer37, and Gly34 are critical for β-TrCP1-β-catenin binding and specificity, while Ile35, which makes fewer contacts, plays a smaller role. This is also reflected in the distribution of β-catenin mutations identified in colorectal, hepatocellular, endometrial, gastric, and ovarian cancers (reviewed in Polakis, 2000). In a recent survey (Polakis, 2000), Asp32, Ser 33, Gly 34, and Ser37 were found mutated in 36, 23, 22 and 30 cases, respectively, while there were only two mutations reported for Ile35.

F Box and Its Interface with Skp1

The β-TrCP1 F box contains the same overall three-helix cluster structure (H1, H2, and H3) seen with the F box of Skp2, but there are several differences (1.5 Å rmsd for 37/42 Cα atoms). While the H1 and H2 helices align well, the H3 helix of β-TrCP1 is tilted further away from the H2 helix by ~15° (Figure 3A). This is due, in part, to the six C-terminal F box residues (residues 187 to 192). While these residues match the F box consensus well in both β-TrCP1 and Skp2, they adopt different structures as they pack with the different linker structures that follow the F boxes (Figure 3B). In β-TrCP1, they form an α helix that continues as the first helix of the helical linker domain, whereas in Skp2 they adopt a coil structure that interacts with the LRR-like linker. A second difference involves the N terminus of the β-TrCP1 F box, which contains a 5 residue insertion (Figures 3A and 3B) that forms an additional α helix (H0; Figure 3A).

The β-TrCP1 F box binds Skp1 through a bipartite interface. One face of the F box interacts with the H5 and H6 helices of the BTB/POZ core and with the H7 helix of Skp1, while the opposite face interacts with the H8 helix. This binding mode is very similar to that seen in the Skp1-Skp2 complex, but the positions of the β-TrCP1 F box and of the Skp1 H7 and H8 helices are shifted together by ~2.0 Å away from the BTB/POZ core of Skp1 (Figure 3C). The rest of the Skp1 structure is essentially identical in the two complexes (0.8 Å rmsd for 102 Cα atoms). The movement of the F box is associated with the β-TrCP1 H0 helix wedging into the expanded space between the BTB/POZ core and one face of the F box (Figure 3C). This plasticity in the F box-Skp1 interface is likely related to the entirely different β-TrCP1 and Skp2 linker structures, which pack with the F box and, in the case of Skp2, with Skp1.

Linker between the F Box and WD40 Domain

The four helices (H4, H5, H6, and H7) of the linker pack into a globular domain that is anchored tightly on the F box and WD40 domains (Figure 1A). The residues that form the first turn of the linker H4 helix correspond to the C terminus of the F box motif, and the linker H7 helix makes additional contacts with the F box (Figure 3D). On the WD40 side, the linker H5 and H7 helices pack with blades 6, 7, and 1 through van der Waals contacts and hydrogen bond networks involving conserved residues (Figure 1C and Supplemental Figure S1 at http://www.molecule.org/cgi/content/full/11/6/1445/DC1).

In the structure of the yeast Skp1-Cdc4 complex, the linker forms a three-helix globular domain (Orlicky et al., 2003). Two of the Cdc4 linker helices have positions and orientations, relative to Skp1, that are very similar to the H4 and H7 helices of the β-TrCP1 linker. These Cdc4 linker helices make contacts to the F box and WD40 domains that are highly analogous to those made by the β-TrCP1 H4 and H7 helices. The β-TrCP1-Skp1 complex thus reinforces the notion that the rigidity of the linkage between the F box and the substrate binding domain is important for SCF function (Schulman et al., 2000).

Model of the $SCF^{\beta\text{-}TrCP1}$-β-Catenin Complex

The structure of the Skp1-β-TrCP1-β-catenin complex makes it possible to construct a model of a substrate-bound SCF by simply superimposing the Skp1-F box portions of the Skp1-β-TrCP1-β-catenin and the SCF^{Skp2} complexes (Zheng et al., 2002). In this $SCF^{\beta\text{-}TrCP1}$ model, the top face of the WD40 domain faces the E2 binding site on Rbx1, and both the N and C termini of the β-catenin peptide point toward Rbx1 (Figure 4). The position of the WD40 domain is remarkably similar to the position of the LRR domain in the SCF^{Skp2} structure, and in the superimposition of the two SCFs roughly half of the WD40 domain structure overlaps the LRR domain (Figure 4). A similar overlap of substrate binding domains has also been reported for the superposition of the yeast Skp1-Cdc4 (Orlicky et al., 2003) with the Skp1-Skp2 structure.

To further explore the significance of this similarity in the positions of the substrate binding domains, we constructed a model of the SCF-like VHL-ElonginB-ElonginC-Cul2-Rbx1 (VBCCR) complex. On the basis of sequence and structure relationships from published

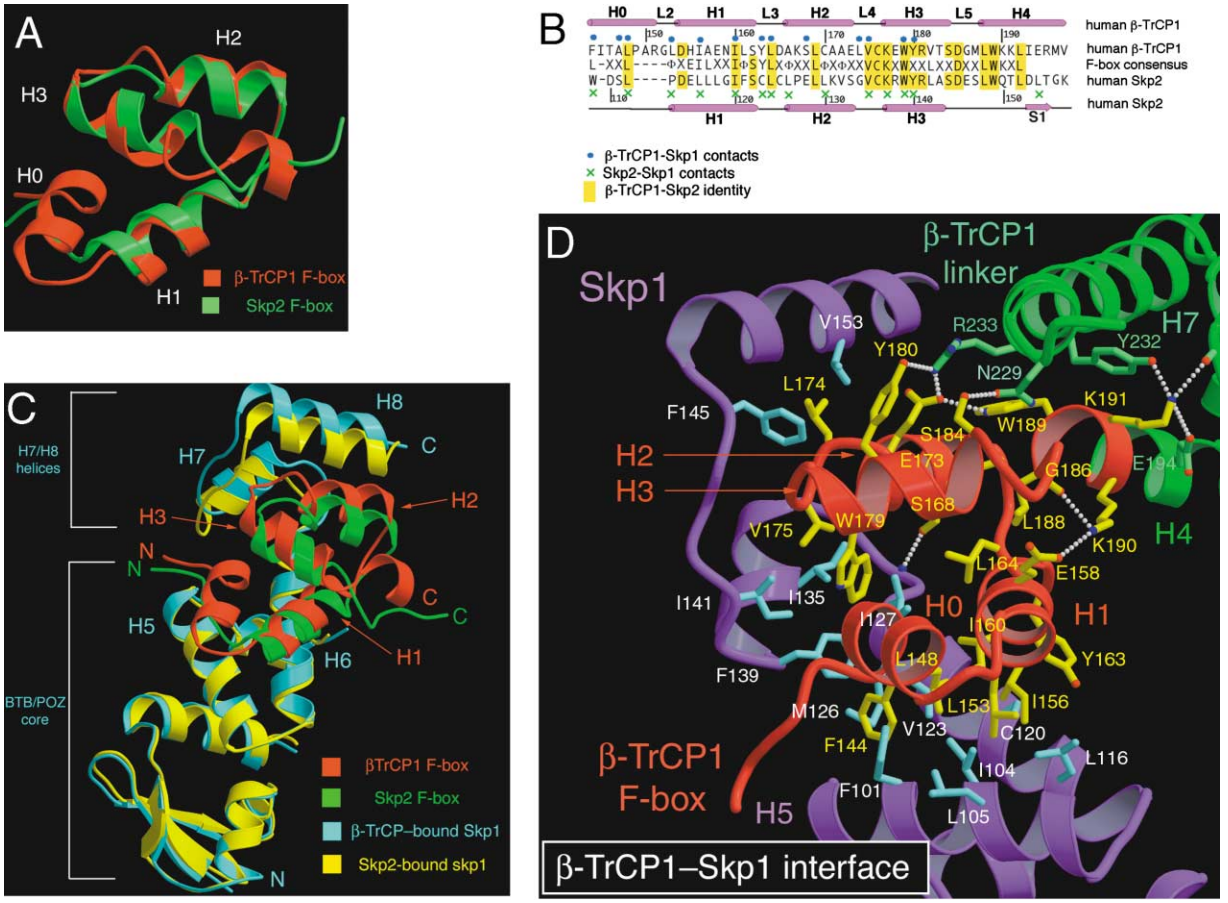

Figure 3. The β-TrCP1-Skp1 Interface Is Similar to that in the Skp1-Skp2 Complex

(A) Superimposition of the β-TrCP1 (red) and Skp2 (green) F boxes. Secondary structure elements of the β-TrCP1 F box are labeled.

(B) Structure-based sequence alignment of the β-TrCP1 and Skp2 F box sequences, and their comparison to the F box motif consensus. The β-TrCP1 and Skp2 secondary structure elements and residue numbers are labeled above and below their sequences, respectively. Identical residues between β-TrCP1 and Skp2 are highlighted in yellow. Skp1-interacting residues in β-TrCP1 are indicated by blue dots, and those in Skp2 are indicated by green crosses.

(C) The β-TrCP1 F box and Skp1 H7-H8 helices are shifted en bloc away from the Skp1 BTB/POZ core compared to the structure of Skp1-Skp2. The structures were superimposed by aligning the BTB/POZ core of Skp1 in the two structures.

(D) Close-up view of the interface between β-TrCP1 and Skp1, showing intermolecular contacts. The β-TrCP1 F box is shown in red, the linker in green, and Skp1 in purple. Side chains of the β-TrCP1 F box (pink), linker (light green), and Skp1 (cyan) that are involved in intermolecular or interdomain contacts are also shown. Hydrogen bonds are represented by white dotted lines.

work (Stebbins et al., 1999; Schulman et al., 2000; Zheng et al., 2000), we superimposed the structurally conserved portions of Skp1 and ElonginC from Cul1-Rbx1-Skp1-F box^{Skp2} and VHL-ElonginB-ElonginC-Hif1α peptide (Min et al., 2002) complexes (Figure 4). The substrate binding domain of VHL (termed β domain) points toward Rbx1, with the N terminus of the Hif1α peptide in sight of Rbx1. The position of the VHL β domain is again very similar to the β-TrCP1 WD40 and Skp2 LRR domains, although it does not extend as far toward Rbx1. The distance from the Hif1α peptide to Rbx1 is ~25 Å longer compared to the SCF$^{β\text{-}TrCP1}$-β-catenin peptide model (Figure 4).

The structure of the E2-Rbx1 complex is unknown, but a model of the SCF^{Skp2} bound to an E2 has been proposed based on the structure of the c-Cbl-E2 complex and on mutagenesis indicating that the Rbx1 RING domain has an E2 binding site similar to that of c-Cbl's RING domain (Zheng et al., 2000). Based on this SCF-E2 model, the E2 active site cysteine would end up ~50 Å away from the structured N- or C-terminal ends of the β-catenin peptide (Figure 4). The SCF-E2 model may have a significant error in the position of the E2 active site, however, as c-Cbl also uses a domain outside its RING to bind the E2, and a counterpart to this is not apparent in the SCF. Pivoting about the E2-Rbx1 interface of the model could significantly affect the final position of the E2 active site, which is ~20 Å away from the E2-Rbx1 interface (Figure 4). For example, a 45° uncertainty in the orientation of the E2 could result in ±20 Å errors in the position of the E2 active site cysteine relative to the SCF.

Ubiquitination Rate Depends on Lysine-Destruction Motif Spacing

The similar positions of the three substrate binding domains supports the current model that the SCF and other RING E3s promote ubiquitin transfer by positioning the

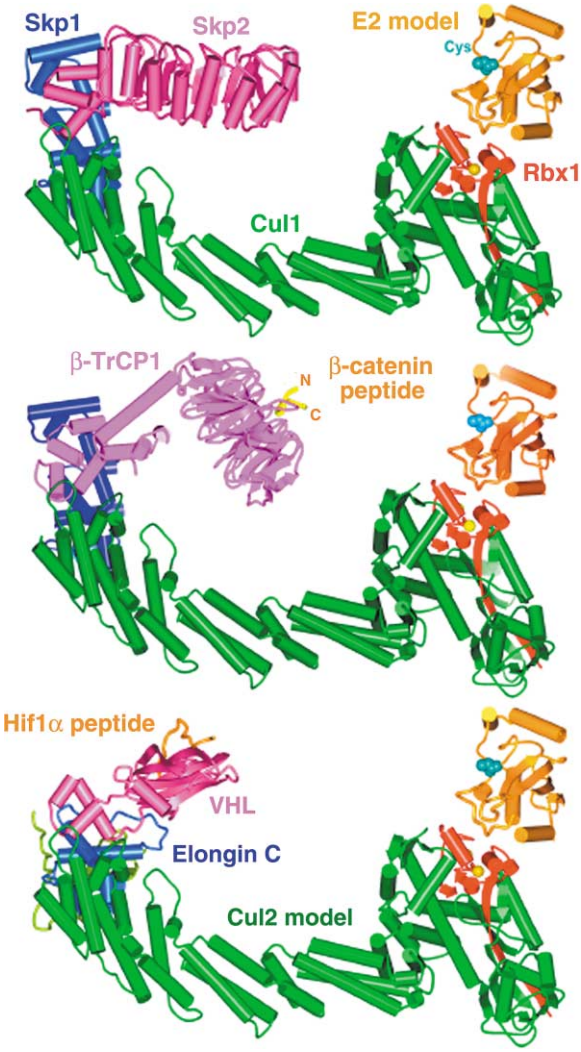

Figure 4. Models of the SCF^{Skp2} (Top), $SCF^{\beta\text{-}TrCP1}$ (Middle), and the SCF-like VBC-CR Complex (Bottom) Bound to E2

The E2 was docked based on the composite structure of the SCF^{Skp2} (Zheng et al., 2002) and on the RING-type E3 c-Cbl bound to the UbcH7 E2 (Zheng et al., 2000). The model of the VBC-CR complex contains a model of Cul2, and a model of the Cul2-ElonginC interface, based on the structure of the VHL-ElonginB-ElonginC-Hif1α peptide complex (Min et al., 2002). The E2 active site cysteine, which would be attached to the ubiquitin C terminus through a thioester bond, is shown in space-filling representation and is colored cyan.

substrate in a manner such that the lysine is optimally presented to the E2 active site (Schulman et al., 2000; Zheng et al., 2000, 2002). One prediction of this positioning model is that the location of the ubiquitinated lysine relative to the destruction motif is important for the efficiency of $SCF^{\beta\text{-}TrCP1}$-mediated ubiquitination. The β-catenin lysine(s) that gets ubiquitinated has not yet been mapped, but in the case of the IκBα substrate, two adjacent lysines (Lys21 and Lys22) have been shown to be necessary and sufficient for ubiquitination and degradation (Scherer et al., 1995; Baldi et al., 1996). These two IκBα lsyines are located 10 and 9 residues upstream of the destruction motif. Inspection of the human β-catenin sequence showed that it contains a lysine (Lys19) 13 residues upstream of the destruction motif (Figure 1C). In addition, all of the IκBα and β-catenin orthologs and paralogues also contain a lysine located 9 to 14 residues upstream of the destruction motif (Table 1).

Table 1. Distance to Nearest Lysine Upstream of Destruction Motif

Substrate	Residues
IκBα (human)	9 and 10
IκBβ (human)	9
IκBε (human)	11
Cactus (fly IκB)	10 and 12
β-catenin (human)	13
Armadillo (fly β-catenin)	14
Bar-1 (worm β-catenin)	10
Plakoglobin (human)	11

We thus tested whether a β-catenin peptide containing Lys19 and the destruction motif can be ubiquitinated in an in vitro reaction reconstituted with E1, E2 (UbcH5), and $SCF^{\beta\text{-}TrCP1}$, all purified to >90% homogeneity. As shown in Figure 5A, the β-catenin peptide is ubiquitinated in an $SCF^{\beta\text{-}TrCP1}$-dependent manner to an overall level comparable to the IκBα substrate peptide (compare lanes 3 and 6). Replacing $SCF^{\beta\text{-}TrCP1}$ with the SCF^{Skp2}-Cks1 complex, which was previously shown to ubiquitinate the $p27^{Kip1}$ substrate in vitro (Zheng et al., 2002), did not produce any detectable ubiquitinated β-catenin, demonstrating that our assay conditions maintain the substrate specificity of the $SCF^{\beta\text{-}TrCP1}$ (Figure 5A, compare lanes 3 and 8). In order to be able to accurately measure the ubiquitination of the β-catenin lysine independent of the ubiquitination of lysine(s) on ubiquitin, we used the R7 ubiquitin mutant that lacks lysines and thus does not form polyubiquitin chains (Zhou et al., 2001). When we use the wild-type ubiquitin instead of the R7 mutant, the reaction yields the expected high-molecular weight polyubiquitinated β-catenin peptide that can be seen by either Coomasie staining or by immunoblotting with anti-β-catenin antibodies (Figure 5B). These findings, together with the conservation of this lysine among β-catenin orthologs and paralogues (Table 1), suggest that Lys19 is a ubiquitination site of β-catenin in vivo.

We next tested a series of mutant β-catenin peptides where the spacing between Lys19 and the destruction motif was altered in 4 residue steps. We decreased the spacing by deleting 4 (residues 21 to 24; wt−4 peptide in Figure 5C) or 8 residues (residues 21 to 28; wt−8) starting at Ala21. We increased the spacing by inserting a Gly-Ser linker of either 4 (wt+4) or 8 (wt+8) residues at the same site (Figure 5C). The deleted residues and the residue where the linkers were inserted are present in the crystallized peptide but are disordered in the structure, indicating that they are not involved in β-TrCP1 binding. The mutations are also unlikely to have long-range structural effects because the N-terminal 133 amino acids that encompass this region have been shown, by proteolytic digestion, to be unstructured (Huber et al., 1997). The ubiquitination assays were performed using a catalytic amount of $SCF^{\beta\text{-}TrCP1}$ (1.9 μM) compared to ubiquitin and peptide substrates (0.2 mM). The mutant and wild-type β-catenin peptides and the

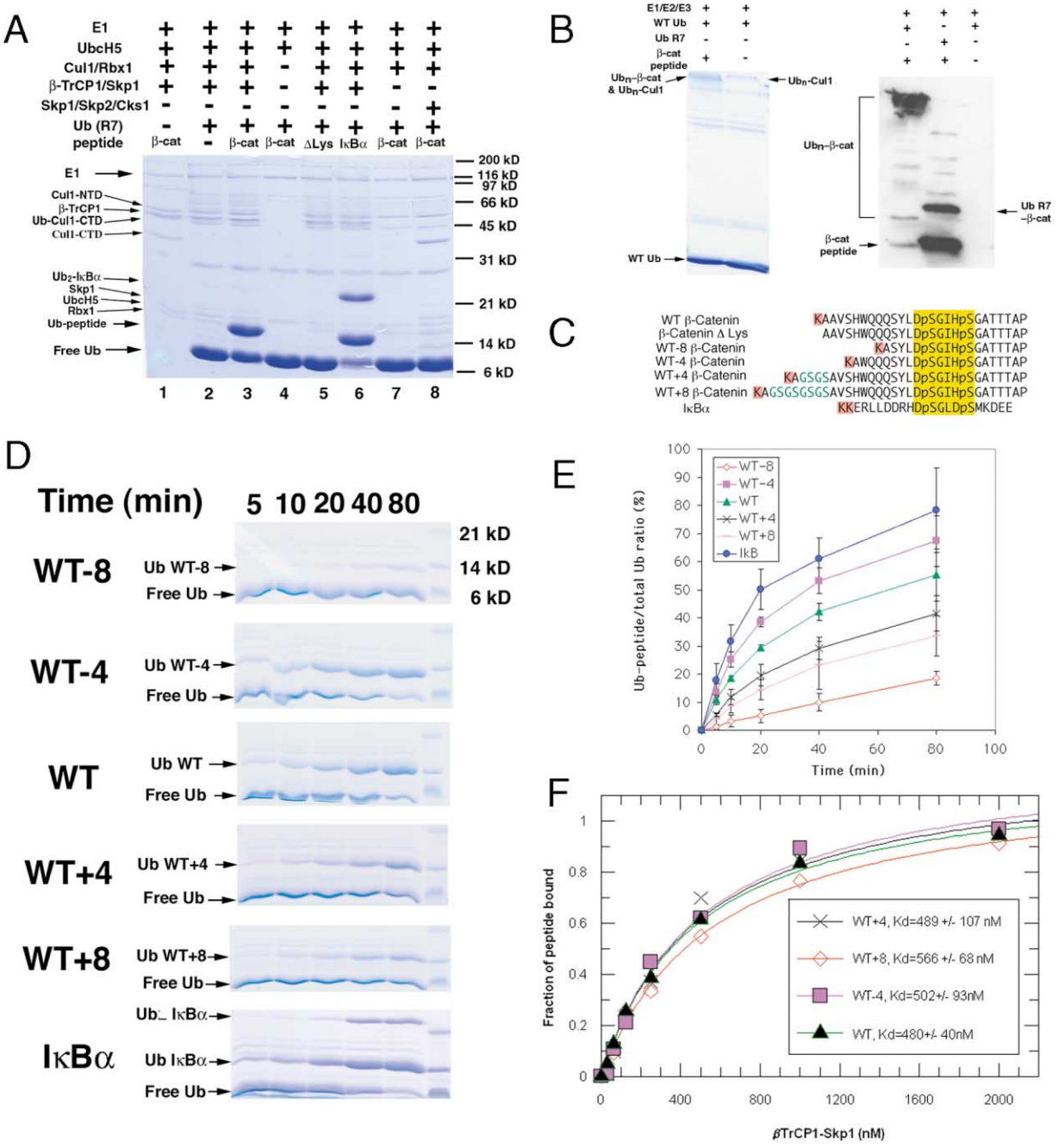

Figure 5. The Rate of Ubiquitination by the $SCF^{\beta\text{-}TrCP1}$ Is Dependent on the Spacing between the Ubiquitination-Site Lysine and the Destruction Motif

(A) The reconstitution of an in vitro ubiquitination system with purified E1, E2, and E3 enzymes. When the R7 mutant of ubiquitin is used, the $SCF^{\beta\text{-}TrCP1}$ monoubiquitinates the doubly phosphorylated β-catenin (lane 3) and IκBα (lane 6) peptides at comparable rates. The reaction is dependent on Lys19 in the β-catenin peptide (lane 5) and is specific for β-TrCP1 because Cul1-Rbx1 (lane 7) or SCF^{Skp2}-Cks1 (lane 8) cannot substitute for $SCF^{\beta\text{-}TrCP1}$. The SDS-PAGE gel was visualized by Coomassie staining. In this system, the Cul1 C-terminal fragment also gets ubiquitinated (Ub-Cul1-CTD).

(B) When wild-type ubiquitin is used, the in vitro system yields high molecular weight polyubiquitinated products. The reaction conditions are identical to those in (A), except for the β-catenin concentration, which is 50-fold less. The gels were visualized either by Coomassie staining (left panel) or by Western blot (right panel) using anti-phospho-β-catenin antibodies (Cell Signaling).

(C) Sequences of the wild-type and mutant β-catenin and IκBα peptides used in the in vitro ubiquitination assay. The destruction motif is highlighted in yellow, the ubiquitinated lysines in pink, and the residues inserted in the wt+4 and wt+8 mutant β-catenin peptides in green.

(D) Ubiquitination of the wt−8, wt−4, wild-type, wt+4, wt+8 β-catenin peptides, and of the wild-type IκBα peptide at different time points. Substrates and products were visualized by Coomassie staining following SDS-PAGE. Bands corresponding to free ubiquitin, ubiquitinated peptides, and doubly ubiquitinated peptides are indicated.

(E) Plot of the ubiquitinated peptide/total ubiquitin ratio as a function of time. All six peptides were assayed at the same time, and each set was repeated four times. The average and standard deviations of four experiments for each peptide are plotted.

(F) Binding of the β-TrCP1-Skp1 complex to the monoubiquitinated wt−4, wild-type, wt+4, and wt+8 β-catenin peptides. The dissociation constants (K_D) and standard deviations of curve fitting are indicated in the inset.

wild-type IκBα peptide were assayed at the same time, in a 5 point time course (Figure 5D). The set of experiments was repeated four times (Figure 5E), and the ordering of the peptides by their ubiquitination efficiency was identical in all repetitions.

We found that changing the Lys19-destruction motif spacing had a significant effect on the ubiquitination rate (Figures 5D and 5E). The wt−8 peptide was the poorest substrate, with only trace amounts of ubiquitinated wt−8 produced at the longer reaction times. The wt+8 peptide was the second poorest substrate, although its ubiquitination rate was closer to the rest of the peptides than to that of wt−8 (Figures 5D and 5E). The wt+4 peptide was ubiquitinated at a rate intermediate between those of the wt+8 and wt peptides, establishing a trend of decreasing rates with increasing spacing. Surprisingly, the ubiquitination rate of the wt−4 peptide was slightly, but consistently, higher than that of the wild-type peptide (Figures 5D and 5E). It is noteworthy that IκBα, where the lysine-destruction motif spacings of 9 and 10 residues is comparable to the 9 residue spacing of the wt−4 mutant, also is a slightly better substrate than wt β-catenin (compare the 5, 10, and 20 min time points, when the majority of the IκBα product is monoubiquitinated, in Figures 5D and 5E).

To experimentally confirm the structure-based conclusion that the insertions and deletions in the β-catenin peptide would not affect the association of the peptides with β-TrCP1, we used a native gel electrophoretic mobility shift assay to measure the binding of the peptides to the Skp1-β-TrCP1 complex. In order to quantitate binding and calculate the dissociation constants (K_D) precisely, we used peptides that have been monoubiquitinated with an R7 ubiquitin tagged with a cAMP-dependent-protein kinase (PKA) site, allowing the labeling with ^{32}P (see Supplemental Figure S2 at http://www.molecule.org/cgi/content/full/11/6/1445/DC1). The K_D values of the Skp1-β-TrCP1 bound to monoubiquitinated wild-type and wt−4, wt+4, and wt+8 mutant β-catenin peptides are indistinguishable, ranging from 480 to 566 nM with standard deviations of 68 to 107 nM (Figure 5F). We could not obtain adequate amounts of the wt−8 monoubiquitinated product to perform this experiment.

These data establish the spacing between the destruction motif and the ubiquitin-acceptor lysine residue as a parameter that affects the rate of substrate ubiquitiation, further supporting the positioning model.

Implications for SCF-Mediated Catalysis of Ubiquitination

The finding that 4 residue changes in the lysine-destruction motif spacing affect the rate of ubiquitination up to ~2-fold, but do not eliminate it, suggests that the positioning effect operates through increasing the effective concentration of the lysine at the E2 active site (Zheng et al., 2002) and not through a more precise mechanism, such as the alignment of the lysine side chain for nucleophilic attack. According to this effective concentration model, a specific SCF will catalyze ubiquitination maximally when the distance between its substrate binding site and the E2 active site, a parameter likely unique to a particular F box protein, closely matches the spatial distance between the substrate's SCF binding motif and its lysine residue. In the case of the β-catenin substrate, the segment between the destruction motif and the lysine is unstructured and as such it would sample a distribution of lengths, instead of having a single, well-defined length. The length distribution of an unstructured polypeptide can be described by an average length and a standard deviation related to how broad the distribution is (Creighton, 1993 and references therein). Except for very short polypeptides, it is not possible to ab initio calculate these parameters with accuracy, especially as the amino acid sequence can significantly affect the distribution. However, statistical approaches based on random polymer theory, which assumes each monomer unit is free to rotate, have been shown to agree with experimental data qualitatively, and can be used to compare relative length distributions of related peptides (Haas et al., 1975; Creighton, 1993).

We applied polymer theory to see whether the observed differences in the ubiquitination rates of the mutant peptides are consistent with the effective concentration model. We compared the wt−4 peptide, which had the highest ubiquitination efficiency in our assay, and the wt+8 peptide, which was ubiquitinated at an approximately 3-fold lower apparent rate. For the wt−4 peptide, we used a random polymer model of 7 units (7-mer) corresponding to the number of residues between the lysine of wt−4 and the first β-catenin residue that is ordered in the crystals (Tyr30). Similarly, we used a model of 19 units for the wt+8 peptide (see Supplemental Figure S3 at http://www.molecule.org/cgi/content/full/11/6/1445/DC1). The average end-to-end distance for the 7-mer was 2.64 monomer units, compared to 4.35 units for the 19-mer. Setting the condition that the distance from β-TrCP1 to the E2 active site matches the average length of the optimal 7-mer, the probability that the 19-mer would sample this distance is lower by a factor of 2.5 (see Supplemental Figure S3). Assuming that the reaction rate is proportional to the fraction of time that the lysine spends near the E2 active site, the predictions of the effective concentration model are thus consistent with the magnitude of the rate effects we observe on varying the lysine-destruction motif distance.

Our experimental data showing that ubiquitination by the $SCF^{\beta\text{-}TrCP1}$ is most efficient when a lysine is present 9 to 13 residues upstream from the destruction motif of the substrate indicates that this is the position that the $SCF^{\beta\text{-}TrCP1}$ maximally concentrates at the E2 active site. Although we cannot calculate the average spatial lengths of these residue spacings, we can put an upper limit, as the wt−4 peptide can reach only ~32 Å in a fully extended conformation of its backbone and lysine side chain. This is shorter than the ~50 Å β-TrCP1-E2 distance in the $SCF^{\beta\text{-}TrCP1}$-E2 model, but we presume it is within the uncertainty in the E2 active site position discussed earlier.

If the lysine-destruction box spacing is smaller than what would minimally be required to reach the E2, the model predicts that it will not be ubiquitinated. Although the wt−8 peptide, which would likely be too short to reach the E2, shows a low level of ubiquitination, this could be due to a fraction of the peptide population

Table 2. Statistics from the Crystallographic Analysis

Data Set	Native	Hg λ1	Hg λ2	Hg λ3
Wavelength (Å)	0.9500	1.0090	1.0080	0.9919
Resolution (Å)	2.95	3.2	3.2	3.2
Observations	52,111	66,393	85,472	69,895
Unique reflections	17,628	15,512	15,522	15,528
Data coverage (%)	99.3	99.4	99.9	99.7
R_{sym} (%) (3.025–2.950 Å)	4.0 (43.0)	5.8 (35.2)	6.5 (28.9)	5.9 (28.7)
MAD Analysis				
Resolution	20–3.6	20–3.4	20–3.4	20–3.4
Phasing power	0.58	–	1.24	1.10
R_{cullis}	0.94	–	0.78	0.81
Anomalous R_{cullis}	–	0.94	0.89	0.91
Mean FOM	0.48			
Refinement Statistics				
Resolution range (Å)		20.0-2.95		
Reflections ($\|F\| > 0\sigma$) (3.025–2.950 Å)		16,793 (1201)		
Total atoms		4340		
R factor (%) (3.025–2.950 Å)		23.0 (43.3)		
R_{free} (%) (3.025–2.950 Å)		28.6 (51.1)		
Rmsd				
Bonds (Å)		0.014		
Angles (°)		1.855		
B factor (Å^2)	Main chain bond	0.649	Side chain bond	2.013

$R_{sym} = \Sigma_h\Sigma_i |I_{h,i} - I_h|/\Sigma_h\Sigma_i I_{h,i}$ for the intensity (I) of i observations of reflection h. Phasing power = $<F_{\lambda i}>/E$, where $<F_{\lambda i}>$ is the rms heavy atom structure factor and E is the residual lack of closure error. R_{cullis} is the mean residual lack of closure error divided by the dispersive or anomalous difference. R factor = $\Sigma||F_{obs}| - |F_{calc}||/\Sigma|F_{obs}|$, where F_{obs} and F_{calc} are the observed and calculated structure factors, respectively. R_{free} = R factor calculated using 5% of the reflection data chosen randomly and omitted from the start of refinement. Rmsd, root-mean-square deviations from ideal geometry and variations in the B factor of bonded atoms.

sampling the vicinity of the E2 through random diffusion, as part of the dynamic binding equilibrium.

In the SCF$^{\beta\text{-TrCP1}}$-β-catenin-E2 model, both the N and C termini of the β-catenin peptide point toward the E2, and they are roughly equidistant from it. This suggests that a lysine C-terminal to the destruction motif could also be ubiquitinated efficiently as long as it matches the distance criteria. Interestingly, β-catenin, armadillo, and plakoglobin all have a lysine located 9 residues C-terminal to the last ordered β-catenin residue, although this lysine is absent in the worm β-catenin ortholog. It is thus conceivable that this is a second ubiquitination site of β-catenin in vivo. This is supported by the observation that mutation of both Lys19 and Lys49, but not of the individual lysines, reduced the ubiquitination of transiently overexpressed β-catenin (Aberle et al., 1997), although it was not determined whether the degradation of endogenous β-catenin requires these lysines.

The effective concentration model also provides a mechanism for the selection of ubiquitin-acceptor lysines by the SCF. The importance of ubiquitination-site specificity in regulation is reinforced by the reversibility of ubiquitination, as well as by ubiquitination being one of many posttranslational modifications that occur at lysine side chains. For example, IκBα can be modified by the ubiquitin-like protein SUMO on the same residues that undergo ubiquitination, and this has been shown to protect IκBα from ubiquitination and destruction (Desterro et al., 1998). And acetylation, which is another common lysine modification, has been shown to block the ubiquitination of the p53 tumor suppressor and the E2F-1 transcription factor (Li and Verma, 2002; Martinez-Balbas et al., 2000).

Our findings thus solidify the model that the SCF catalyzes ubiquitination by increasing the effective concentration of the lysine at the active site of the E2, and they also provide a mechanistic basis for the selection of lysine(s) by the SCF.

Experimental Procedures

Protein Expression and Purification

The human β-TrCP1-Skp1 complex was produced by coexpressing the two proteins in insect cells from separate baculoviruses. Residues 139 to 569 of β-TrCP1 were expressed as a glutathione S transferase (GST) fusion protein, and full-length Skp1 with two internal deletions of residues 38 to 43 and 71 to 82 (Schulman et al., 2000) was expressed as an untagged protein. The complex was first purified by glutathione affinity chromatography, and following cleavage of GST by thrombin, by cation exchange and gel filtration chromatography. The β-TrCP1-Skp1 complex was then concentrated to ~15 mg/ml by ultrafiltration in 10 mM BTP, 200 mM NaCl, 5 mM dithiothreitol (DTT) (pH 6.8). The doubly phosphorylated β-catenin and IκBα wild-type and mutant peptides were synthesized chemically and purified by reversed phase chromatography.

Crystallization and Data Collection

The purified β-TrCP1-Skp1 complex (15 mg/ml) and β-catenin peptide (5 mg/ml) were mixed at a 1:2 molar ratio. Crystals of the ternary complex were grown at room temperature by the hanging drop vapor diffusion method by mixing the complex with an equal volume of reservoir solution containing 16%–20% PEG 4000, 320 mM sodium citrate, and 100 mM BTP (pH = 6.8). The crystals form in space group $P3_1$, with a = b = 82.6 Å, c = 111.5 Å, and contain one complex in the asymmetric unit. The native data set was collected at the F1 beamline (λ = 0.950 Å) of the Cornell High Energy Synchrotron Source (MacCHESS) using crystals flash-frozen in crystallization

buffer supplemented with 20% ethylene glycol at −170°C (Table 2). For the multiwavelength anomalous diffraction (MAD) data sets, crystals were soaked in 0.2 mM thimerosal for 1.5 hr before being frozen. Reflection data were indexed, integrated, and scaled using DENZO and SCALEPACK (Otwinowski and Minor, 1997).

Structure Determination and Refinement

The structure of the complex was determined by a combination of molecular replacement and multiwavelength anomalous diffraction (MAD) using a Hg derivative. The initial MAD phases were improved by density modification with the program DM (CCP4, 1994). Molecular replacement with the program AmoRe (CCP4, 1994) was used to locate the Skp1 and WD40 portions of the complex with search models consisting of Skp1 (Schulman et al., 2000) and the Gβ WD40 domain (Sondek et al., 1996), respectively. The initial model was built with the program O (Jones et al., 1991) and was improved by several cycles of manual rebuilding and refinement with the programs CNS (Brunger et al., 1998) and REFMAC (CCP4, 1994). The refined model contains residues 139 to 217 and 227 to 545 of β-TrCP1, residues 2 to 37, 44 to 65, and 85 to 160 of Skp1, and residues 30 to 40 of β-catenin. Residues 218 to 226 and 546 to 569 of β-TrCP1; residues 66 to 70, 83 to 84, and 161 to 163 of Skp1; and residues 19 to 29 and 41 to 44 of β-catenin are not visible in the electron density maps and are presumed to be disordered. Coordinates have been deposited in the RCSB Protein Data Bank under code 1P22.

In Vitro Ubiquitination Assay of Full-Length IκBα by the In Vitro Translated β-TrCP1 Mutants

IκBα ubiquitination assays were performed at 30°C (1 hr) in a total volume of 15 μl containing 50 ng His_6-E1 purified from budding yeast, 500 ng bacterial His_6-Cdc34, 4 mM ATP, 10 μg of ubiquitin, 1 μM ubiquitin-aldehyde, 1 μg of IκBα/NFκB complex previously phosphorylated with IKK (Winston et al., 1999a), 20 μM LLNL (Sigma), 9 μl of reticulocyte lysate containing in vitro translated β-TrCP1 proteins or control reticulocyte extracts lacking β-TrCP1, 25 mM Tris-HCl (pH 8.0), and 10 mM magnesium chloride. Reaction mixtures were separated by SDS-PAGE and IκBα detected by Western blotting using polyclonal antibodies against IκBα (Santa Cruz).

In Vitro Ubiquitination Assay of β-Catenin and IκBα Peptides

The R7 mutant of ubiquitin was expressed with an N-terminal His_6 tag and purified by Ni-NTA chromatography. Human E1 was expressed in insect cells as a GST-fusion protein and was purified by glutathione affinity chromatography. Human UbcH5, expressed as a GST-fusion protein in *E. coli*, was purified by glutathione affinity chromatography, followed by thrombin cleavage, cation exchange, and gel filtration chromatography. The human Cul1-Rbx1 complex used in the assays consists of the noncovalently associated N- and C-terminal domains of Cul1 (NTD and CTD) and Rbx1 (Zheng et al., 2002). The split Cul1, which allows the production of the Cul1-Rbx1 complex in a soluble form in *E. coli*, was previously shown to have the same structure as the insect cell-produced intact Cul1-Rbx1 complex and to assemble with the Skp1-Skp2-Cks1 to ubiquitinate $p27^{Kip1}$ in vitro (Zheng et al., 2002). All proteins were purified to >90% homogeneity. Purified E1 (670 nM), UbcH5 E2 (2.6 μM), Cul1 (NTD+CTD)-Rbx1 (1.9 μM), β-TrCP1-Skp1 (1.9 μM), Ub R7 (200 μM), and the substrate peptides (170 μM) were mixed in a solution supplemented with 10 mM ATP and 20 mM $MgCl_2$ in a total volume of 10 μl, and were incubated at room temperature for 30 min or as indicated. The reaction was stopped by mixing with 2× SDS loading buffer, was analyzed by SDS-polyacrylamide gel electrophoresis, and was visualized by Coomassie staining. The amounts of ubiquitinated peptides and free ubiquitin were quantitated, and the average and standard deviation were calculated and plotted with Microsoft Excel.

Dissociation Constants of β-TrCP1-Skp1-β-Catenin Complexes

The R7 mutant of ubiquitin was tagged with an N-terminal cAMP-dependent-protein kinase (PKA) site followed by a His_6 tag (referred to as PKA-Ub-R7). It was expressed in *E. coli* and was purified by Ni-NTA affinity and cation exchange chromotography. The wild-type, wt−4, wt+4, wt+8 β-catenin peptides were conjugated to PKA-Ub-R7 by scaling up the reaction described above. The PKA-Ub-R7-β-catenin peptides were purified from the reaction mixture by Ni-NTA affinity and cation exchange chromatography, and were ^{32}P labeled using ^{32}P-ATP and PKA (Sigma). ^{32}P-PKA-Ub-R7-β-catenin peptides (10 nM) were incubated with various concentrations (from 31 nM to 2 μM) of purified β-TrCp1-Skp1 in a final volume of 8 μl on ice for 30 min. The free and bound peptides were separated by native-gel electrophoresis using 4.8% polyacrylamide gels in TBE buffer, and visualized by phosphorimager analysis. The free and β-TrCp1-Skp1-bound peptides were quantitated using the program MacBas. The data were fitted into the quadratic equation of the binding equilibrium with the program GraFit to obtain K_D values and standard deviations (Figure 5F).

Acknowledgments

We thank the staff of the Cornell High Energy Synchrotron Source MacChess and of the National Synchrotron Light Source X9A beamlines for help with data collection. This work was supported by the NIH, the Howard Hughes Medical Institute, the Dewitt Wallace Foundation, the Samuel and May Rudin Foundation, and the Arthur and Rochelle Belfer Foundation.

Received: January 24, 2003
Revised: April 14, 2003
Accepted: April 25, 2003
Published: June 19, 2003

References

Aberle, H., Bauer, A., Stappert, J., Kispert, A., and Kemler, R. (1997). β-catenin is a target for the ubiquitin-proteasome pathway. EMBO J. *16*, 3797–3804.

Bai, C., Sen, P., Hofmann, K., Ma, L., Goebl, M., Harper, J.W., and Elledge, S.J. (1996). Skp1 connects cell cycle regulators to the ubiquitin proteolysis machinary through a novel motif, the F-box. Cell *86*, 263–274.

Baldi, L., Brown, K., Franzoso, G., and Siebenlist, U. (1996). Critical role for lysines 21 and 22 in signal-induced, ubiquitin-mediated proteolysis of IκBα. J. Biol. Chem. *271*, 376–379.

Brunger, A.T., Adams, P.D., Clore, G.M., DeLano, W.L., Gros, P., Grosse-Kunstieve, R.W., Jiang, J.S., Kuszewski, J., Nilges, M., and Pannu, N.S. (1998). Crystallography and NMR system: a new software suite for macromolecular structure determination. Acta Crystallogr. D *54*, 905–921.

CCP4 (Collaborative Computational Project 4) (1994). The CCP4 suite: programs for protein crystallography. Acta Crystallogr. D *50*, 760–763.

Creighton, T.E. (1993). Proteins: structures and molecular properties (New York: W.H. Freeman and Company), pp. 176–179.

Deshaies. R.J. (1999). SCF and Cullin/Ring H2-based ubiquitin ligases. Annu. Rev. Cell Dev. Biol. *15*, 435–467.

Desterro, J.M., Rodriguez, M.S., and Hay, R.T. (1998). Mol. Cell *2*, 233–239.

Feldman, R.M., Correll, C.C., Kaplan, K.B., and Deshaies, R.J. (1997). A complex of Cdc4p, Skp1p, and Cdc53p/cullin catalyzes ubiquitination of the phosphorylated CDK inhibitor Sic1p. Cell *91*, 209–219.

Gaudet, R., Bohm, A., and Sigler, P.B. (1996). Crystal structure at 2.4 Å resolution of the complex of transducin βγ and its regulator, phosducin. Cell *87*, 577–588.

Hart, M., Concordet, J.P., Lassot, I., Albert, I., del los Santos, R., Durand, H., Perret, C., Rubinfeld, B., Margottin, F., Benarous, R., and Polakis, P. (1999). The F-box protein β-TrCP associates with phosphorylated β-catenin and regulates its activity in the cell. Curr. Biol. *9*, 207–210.

Haas, E., Wilchek, M., Katchalski-Katzir, E., and Stenberg, I.Z. (1975). Distribution of end-to-end distances of oligopeptide in solution as estimated by energy transfer. Proc. Natl. Acad. Sci. USA *72*, 1807–1811.

Hershko, A., and Ciechanover, A. (1998). The ubiquitin system. Annu. Rev. Biochem. *67*, 425–479.

Hon, W.-C., Wilson, M.I., Harlos, K., Claridge, T.D.W., Schofield, C.J., Pugh, C.W., Maxwell, P.H., Ratcliffe, P.J., Stuart, D.I., and Jones, E.Y. (2002). Structural basis for the recognition of hydroxyproline in HIF-1α by pVHL. Nature *417*, 975–978.

Huber, A.H., Nelson, W.J., and Weis, W.I. (1997). Three-dimensional structure of the armadillo repeat region of β-catenin. Cell *90*, 871–882.

Ivan, M., and Kaelin, W.G., Jr. (2001). The von-Hippel-Lindau tumor suppressor protein. Curr. Opin. Genet. Dev. *11*, 27–34.

Joazeiro, C.A., Wing, S.S., Huang, H., Leverson, J.D., Hunter, T., and Liu, Y.C. (1999). The tyrosine kinase negative regulator c-Cbl as a RING-type, E2-dependent ubiquitin-protein ligase. Science *286*, 309–312.

Jones, T.A., Zou, J.Y., Cowan, S.W., and Kjeldgaard, M. (1991). Improved methods for building protein models in electron density maps and the location of errors in these models. Acta Crystallogr. A *47*, 110–119.

Kipreos, E.T., and Pagano, M. (2000). The F-box protein family. Genome Biol. *1*, 3002.1–3002.7.

Kraulis, P.J. (1991). MOLSCRIPT: a program to produce both detailed and schematic plots of protein structures. J. Appl. Crystallogr *24*, 946–950.

Latres, E., Chiaur, D.S., and Pagano, M. (1999). The human F box protein β-TrCP associates with the Cul1/Skp1 complex and regulates the stability of β-catenin. Oncogene *18*, 849–854.

Li, Q., and Verma, I.M. (2002). NF-kappaB regulation in the immune system. Nat. Rev. Immunol. *2*, 725–734.

Martinez-Balbas, M.A., Bauer, U.M., Nielsen, S.J., Brehm, A., and Kouzarides, T. (2000). Regulation of E2F1 activity by acetylation. EMBO J. *19*, 662–671.

Min, J.-H., Yang, H., Ivan, M., Gertler, F., Kaelin, W.G.,Jr., and Pavletich, N.P. (2002). Structure of an HIF-1α-pVHL complex: hydroxyproline recognition in signaling. Science, *296*, 1886–1889.

Orlicky, S., Tang, X., Willems, A., Tyers, M., and Sicheri, F. (2003). Structural basis for phosphodependent substrate selection and orientation by the SCF^{Cdc4} ubiquitin ligase. Cell *112*, 243–256.

Otwinowski, Z., and Minor, W. (1997). Processing of x-ray diffraction data collected in oscillation mode. Methods Enzymol. *276*, 307–326.

Pickart, C.M. (2001). Mechanisms underlying ubiquitination. Annu. Rev. Biochem. *70*, 503–533.

Polakis, P. (1999). The oncogenic activation of β-catenin. Curr. Opin. Genet. Dev. *9*, 15–21.

Polakis, P. (2000). Wnt signaling and cancer. Genes Dev. *14*, 1837–1851.

Scherer, D.C., Brockman, J., Chen, Z., Maniatis, T., and Ballard, D. (1995). Signal-induced degradation of IκBα requires site-specific ubiquitination. Proc. Natl. Acad. Sci. USA *92*, 11259–11263.

Schulman, B.A., Carrano, A.C., Jeffrey, P.D., Bowen, Z., Kinnucan, E.R.E., Finnin, M.S., Elledge, S., Harper, J.W., Pagano, M., and Pavletich, N. (2000). Insights into SCF ubiquitin ligases from the structure of the Skp1-Skp2 complex. Nature *408*, 381–386.

Skowyra, D., Craig, K.L., Tyers, M., Elledge, S., J., and Harper, J.W. (1997). F-box proteins are receptors that recruit phosphorylated substrates to the SCF ubiquitin-ligase complex. Cell *91*, 209–219.

Skowyra, D., Koepp, D.M., Kamura, T., Conrad, M.N., Conaway, R.C., Conaway, J.W., Elledge, S.J., and Harper, J.W. (1999). Reconstitution of G1 cyclin ubiquitination with complexes containing SCF^{Grr1} and Rbx1. Science *284*, 662–665.

Sondek, J., Bohm, A., Lambright, D.G., Hamm, H.E., and Sigler, P.B. (1996). Crystal structure of a G_A protein βγ dimer at 2.1 Å resolution. Nature *379*, 369–374.

Sprague, E.R., Redd, M.J., Johnson, A.D., and Wolberger, C. (2000). Structure of the C-terminal domain of Tup1, a corepressor of transcription in yeast. EMBO J. *19*, 3016–3027.

Stebbins, C.E., Kaelin, W.G., Jr., and Pavletich, N. (1999). Structure of the VHL-EloginC-ElonginB complex: implications for VHL tumor suppressor function. Science *284*, 455–461.

Wall, M.A., Coleman, D.E., Lee, E., Injuguez-Lluhi, J.A., Posner, B.A., Gilman, A.G., and Sprang, S.R. (1995). The structure of the protein heterotrimer Gi α1β1γ2. Cell *83*, 1047–1058.

Winston, J.T., Strack, P., Beer-Romero, P., Chu, C.Y., Elledge, S.J., and Harper, J.W. (1999a). The $SCF^{β\text{-}TrCP}$-ubiquitin ligase complex associates specifically with phosphorylated destruction motifs in IκBα and β-catenin and stimulates IκBα ubiquitination in vitro. Genes Dev. *13*, 270–283.

Winston, J.T., Koepp, D.M., Zhu, C., Elledge, S.J., and Harper, J.W. (1999b). A family of mammalian F-box proteins. Curr. Biol. *9*, 1180–1182.

Yaron, A., Hatzubai, A., Davis, M., Lavon, I., Amit., S., Manning, A.M., Andersen, J.S., Mann, M., Mercurio, F., and Ben-Neriah, Y. (1998). Identification of the receptor component of the IκBα-ubiquitin ligase. Nature *396*, 590–594.

Zheng, N., Wang, P., Jeffrey, P.D., and Pavletich, N.P. (2000). Structure of a c-Cbl-UbcH7 complex: RING domain function in ubiquitin-protein ligases. Cell *102*, 533–539.

Zheng, N., Schulman, B.A., Song, L., Miller, J.J., Jeffrey, P.D., Wang, P., Chu, C., Koepp, D.M., Elledge, S.J., Pagano, M., et al. (2002). Structure of the Cul1-Rbx1-Skp1-F box^{Skp2} SCF ubiquitin ligase complex. Nature *416*, 703–709.

Zhou, C., Seibert, V., Geyer, R., Rhee, E., Lyapina, S., Cope, G., Deshaies, R.J., and Wolf, D.A. (2001). The fission yeast COP9/signalosome is involved in cullin modification by ubiquitin-related Ned8p. BMC Biochemistry *2*, 7–18.

Accession Numbers

Coordinates have been deposited in the RCSB Protein Data Bank under code 1P22.